# DISPERSION RELATIONSHIPS AND FORM FACTORS OF ELEMENTARY PARTICLES

P. S. Isaev

The survey is devoted to the modern state-of-the-art in the field of the form factors of $\pi$-mesons, K-mesons, and nucleons. The concept of form factors of elementary particles is presented, as well the description of the form factors using dispersion relations; an interpretation of experimental data on the scattering of electrons by pions and nucleons is given by introducing form-factor functions; the theoretical aspects of the link between the difference in masses of charged and neutral K-mesons and the form factors of K-mesons are considered; the various representations of form-factor functions are treated.

## INTRODUCTION*

The subject of the present review is connected with one of the fundamental problems in the physics of elementary particles which is being actively investigated at present – the problem of the structure of elementary particles. The idea that the investigated objects – elementary particles – must have a definite structure is not new. This was discussed from the instant the electron was discovered. However, at present the notion of "structure of elementary particles" has a deeper content than the first concepts of the structure of an electron which were discussed in the beginning of the twentieth century in the papers by Abragam, Lorentz, Poincaré, etc.

The review expounds in simple form the notion of the form factors of elementary particles, the link between form factors and the structure of particles, the description of form factors by means of dispersion relations, and the interpretation of experimental data on the scattering of electrons by pions and nucleons through the introduction of pion and nucleon form factors. There is an enormous number of papers devoted to all of these problems. Here I shall mention only a series of surveys [1-4] to which the reader should refer to obtain a more thorough familiarity with the history of the subject.

Before going over to the review itself, let me make several comments on the method of dispersion relations. At present the method of dispersion relations is one of the reliable methods in field theory and is being used with success to explain experimental data. Right now there is not a single case of contradiction between the dispersion relations and experimental data.

Regrettably, there are also no rigorous experimental proofs of the validity of the method. The existence of dispersion relations was first proved theoretically by N. N. Bogolyubov for scattering of $\pi$-mesons by nucleons in 1956 in his report to the International Convention of Theoretical Physicists in Seattle (see also [5]). Later the existence of dispersion relations was also proved for several other processes involving the interaction of elementary particles. Obtaining such proof (theoretically) is a very difficult matter. At present it is assumed that the dispersion relations are valid for any process. In the present review it is likewise assumed throughout that the use of the dispersion relations is valid for describing the form factors of elementary particles.

*The basis of the present review is a series of lectures read by the author in the International School on the Physics of Elementary Particles at Herzeg Novi (Yugoslavia) in 1966 and published in the book "Methods in Subnuclear Physics," Vol. II, Gordon and Breach, New York (1968). The lectures were published only in English. The text of the lectures was reexamined for the purpose of the present review and was considerably augmented with new material on the investigation of electromagnetic form factors of $\pi$- and K-mesons and nucleons (published during the period from 1966 to 1970).

Joint Institute for Nuclear Research, Dubna. Translated from Problemy Fiziki Élementarnykh Chastits i Atomnogo Yadra, Vol. 2, No. 1, pp. 67-104, 1971.

© 1972 Consultants Bureau, a division of Plenum Publishing Corporation, 227 West 17th Street, New York, N. Y. 10011. All rights reserved. This article cannot be reproduced for any purpose whatsoever without permission of the publisher. A copy of this article is available from the publisher for $15.00.

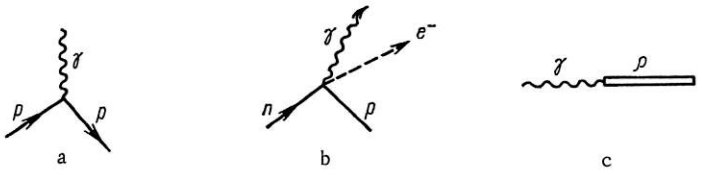


Fig. 1. Feynman diagrams of the simplest vertex functions.

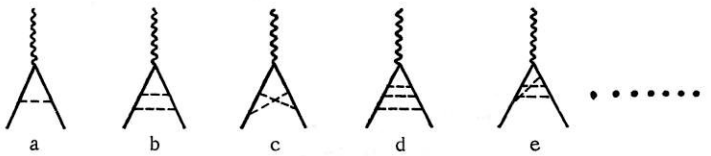


Fig. 2. The different Feynman diagrams which make a contribution to the generalized vertex function displayed in Fig. 3.

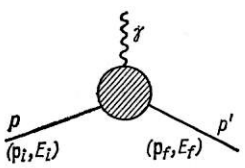


Fig. 3

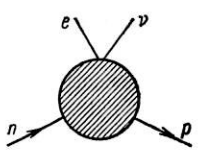


Fig. 4

Fig. 3. Generalized vertex function.

Fig. 4. Generalized vertex function corresponding to the decay $n \to p + e + \nu$.

## 1. THE FORM FACTORS OF ELEMENTARY PARTICLES

No unified definition of the notion of a form factor exists; in the majority of cases it is identified with the notion of a vertex function.

For interaction of an electromagnetic field with nucleons (or $\pi$-mesons) a vertex develops (Fig. 1a). Weak interactions have a vertex of the type depicted in Fig. 1b. The interaction of an electromagnetic field with a p-meson is described by the vertex displayed in Fig. 1c. The interaction force is characterized by coupling constants. Let us consider the three-particle form of interaction (Fig. 1a). We shall include only photons, $\pi$-mesons, and nucleons in the consideration. The experimental data indicates that the constant for coupling of a $\pi$-meson field with a nucleon field is $G^2/4\pi \approx 15$, while the constant for coupling of an electromagnetic field with nucleons is $e^2/\hbar c = 1/137$. Therefore, in describing the interaction of an electromagnetic field with a nucleon ($\pi$-meson) field it is necessary to remember strong coupling of nucleons ($\pi$-mesons) with the $\pi$-meson field (nucleon field). From this the vertex depicted in Fig. 1a must be augmented by a finite collection of diagrams displayed in Fig. 2, in which the $\pi$-mesons are depicted by a dashed line. Symbolically this collection of diagrams together with the diagram described in Fig. 1a may be depicted by a single diagram (Fig. 3) in which the hatched circle denotes the contribution of all possible diagrams allowed by the corresponding interaction Lagrangian. If one of the ends of the diagram (see Fig. 3) is a virtual $\gamma$-quantum ($q^2 \neq 0$), while the other two ends describe a free nucleon, then the vertex function F displayed in Fig. 3 will depend on a single variable $q^2$: namely, $F = F(p^2 = M^2, p'^2 = M^2, q^2 \neq 0)$. Such a function $F(M^2, M^2, q^2)$ is called the electromagnetic form factor of a nucleon. Actually, the interaction of a proton or neutron with a photon can be described by means of two form-factor functions rather than by one, as is shown here for purposes of clarity. This will be considered in greater detail further on.

Methods of summing the infinite number of diagrams displayed in Fig. 3 do not exist, and the form factors are calculated only approximately.

The form factors are also introduced in the case of vertices which describe weak interactions (see Fig. 1b). For example, in the decay $n \to p + e + \nu$ (Fig. 4) the hatched circle denotes consideration of all corrections which occur due to strong interactions of a neutron and proton, while the functions $F(M_n^2, M_p^2, q^2)$ describing these interactions, where the variable quantity $q^2$ is the difference between the four-dimensional proton and neutron momenta, are likewise called form factors, although in the case given all four particles (n, p, e, $\nu$) lie on the mass surface. The name form factor (the electromagnetic form factor of a $\pi$-meson or the $\pi$-meson form factor of bosons, etc.) is linked to the virtual particle according to whose

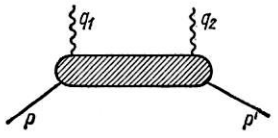


Fig. 5. Representation of the generalized Feynman diagram corresponding to the virtual Compton-effect.

4-momentum the dependence of the form factor is investigated, and to those real particles with which the given virtual particle forms the vertex.

In the case of interaction of one virtual photon with a nucleon the electric charge may be included in the form-factor function in such a way that the "new charge" e' will be related to the conventional charge e by the equation

$$e'(q^2)=F(q^2); \quad e'(0)=F(0)=e, \tag{1}$$

i.e., it is as if a theory were to be obtained with an interaction constant which depends on the transfer of 4-momentum $q^2 = (p'-p)^2$. However, one cannot always represent the form factor function as a variable charge. This can easily be seen if one goes over to more complex diagrams. Considering, for example, a diagram with two virtual ends (Fig. 5), one can see that it may be described by a collection of functions $F_i(q_1^2, q_2^2)$ which will depend in a complex manner on the two variables $q_1^2 \neq 0$ and $q_2^2 \neq 0$, in connection with which neither of them may be interpreted in the spirit of Eq. (1). In the examples considered the collection of functions $F_i(q_1^2, q_2^2)$ describes the amplitudes of the virtual Compton-effect. The form-factor function may not be interpreted as the real space distribution of the electric charge of a nucleon (or of the actual nucleon matter). This derives from the fact that F(x) is a four-dimensional Fourier transform of the function $F(q^2)$:

$$F(x) \sim \int d^4q e^{iqx} F(q^2)$$

and is not associated with the dimensions of the nucleon. It is only for a special selection of the coordinate system for small transfers $q^2$ on the assumption that $F(q^2)$ is a smoothly varying function and for a corresponding definition of the distribution density of the electric charge that one can indicate a link between form factor function $F(q^2)$ and the mean-square radius of a nucleon $\langle r^2 \rangle$ (see, for example, [2]):

$$F(q^2)=F(0)\left[1+\frac{1}{6}\mathbf{q}^2\langle r\rangle^2+\ldots\right], \tag{2}$$

where $\mathbf{q}^2$ is the three-dimensional transfer $(\mathbf{p}'-\mathbf{p})^2$, and F(0) = e.

The form factors may be interpreted most accurately as the influence of the virtual particle clouds on the process amplitude of interest to us (or on the matrix elements of interest to us). Thus, the form factor depicted in Fig. 3 can be interpreted as the effect of the $\pi$-meson virtual cloud of a nucleon on the electromagnetic interaction of the nucleon.

The practical necessity of resorting to form factors to explain experimental data develops fairly frequently. They are also introduced to explain the electromagnetic interaction of particles with nucleons, and in describing weak interactions with allowance for electromagnetic and strong interactions.

In the present review the concept of a "form-factor function" will be used only for electromagnetic vertices (Fig. 1a) when one end of the vertex is a virtual $\gamma$-quantum and the two other ends certainly lie on the mass surface (i.e., the concept of a form factor will be used only for electromagnetic interactions of elementary particles).

The functions $F_i(q_1^2, q_2^2)$ which characterize the amplitudes of the virtual Compton-effect (see Fig. 5) or the functions $F_i(M_n^2, M_p^2, q^2)$ describing the process of neutron decay $n \to p + e + \nu$ (see Fig. 4) will be called relativistic structural coefficients.

In field theory form-factor functions appear for consideration of invariant properties of vertex functions. Thus, the electromagnetic form factor of a $\pi$-meson appears for consideration of a $\pi$-meson vertex (Fig. 6). It may be shown that the sole nonzero vector has the form

$$\langle \pi_2 | j_\lambda | \pi_1 \rangle = \frac{(\pi_1+\pi_2)_\lambda}{\sqrt{4\omega_1\omega_2}} F_\pi(t)\, T_3,$$

where $t = (\pi_2 - \pi_1)^2$; $\omega^2 = \nu + m_\pi^2$; $m_\pi$ is the $\pi$-meson mass; $\nu$ is the square of the three-dimensional $\pi$-meson momentum; $\nu_i = q_i^2$, $\omega_{1,2}$ are the $\pi$-meson energies in the initial and final states, respectively; $T_3$

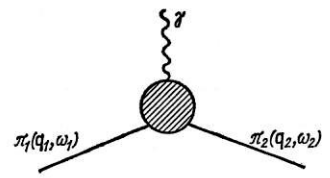


Fig. 6. Generalized π-meson vertex function.

is the third component of the isotopic π-meson spin, while $F_\pi(t)$ is a scalar function of the invariant variable t. At the point t = 0 the function $F_\pi(t)$ is normalized to the electric charge $F_\pi(0) = e$. The expression on the right side of the equation given above is the most general one satisfying the requirements of relativistic invariance. A nucleon vertex has a more complicated form (see Fig. 3), which is associated with the presence of nucleon spin and isotopic spin. Taking account of invariance relative to Lorentz transformations, gauge invariance, and the requirement that free nucleons must satisfy the Dirac equation, and simultaneously considering the isotopic structure, we find that the most general expression for the matrix element of the nucleon current $j_\lambda^N$ has the form

$$\langle p' | j_\lambda^N | p\rangle = \frac{1}{\sqrt{4E_f E_i}} \langle \bar{w}(p') | (F_1^s(t) + F_1^v(t)\tau_3)\gamma_\lambda + i(F_2^s(t) + F_2^v(t)\tau_3)\sigma_{\lambda\nu}k_\nu | w(p)\rangle, \tag{3}$$

where $\bar{w}(p')$ and w(p) are the nucleon spinors in the final and initial states; $E_f$, $E_i$ are the nucleon energies in the final and initial states; the symbols s and v denote the isotopically scalar part and the isotopically vector part of the form factor functions of the nucleon; $\sigma_{\lambda\nu} = \gamma_\lambda\gamma_\nu - \gamma_\nu\gamma_\lambda$, $k_\nu = (p' - p)_\nu$, $t = k_\nu^2$, and, finally, $\tau_3 = \begin{pmatrix} 1 & 0 \\ 0 & -1 \end{pmatrix}$.

The first term in Eq. (3)

$$\langle \bar{w}(p') | (F_1^s(t) + F_1^v(t)\tau_3)\gamma_\lambda | w(p)\rangle = \langle \bar{w}(p') | F_1(t)\gamma_\lambda | w(p)\rangle$$

describes the electromagnetic interaction of a nucleon with a charge e and a magnetic moment equal to the Bohr magneton in the absence of a meson cloud. For t → 0 this term describes the motion of a free noninteracting proton, and therefore it is assumed equal to $e(\bar{w}(p')\gamma_\lambda w(p))$, whence it follows that for a proton

$$F_{1p}(0) = F_1^s(0) + F_1^v(0) = e,$$

while for a neutron

$$F_{1n}(0) = F_1^s(0) - F_1^v(0) = 0$$

or

$$F_1^s(0) = F_1^v(0) = \frac{e}{2}.$$

The second term in Eq. (3)

$$i\langle \bar{w}(p') | (F_2^s(t) + F_2^v(t)\tau_3)\sigma_{\lambda\nu}k_\nu | w(p)\rangle = i\langle \bar{w}(p') | F_2(t)\sigma_{\lambda\nu}k_\nu | w(p)\rangle$$

is associated with an anomalous nucleon magnetic moment. Sometimes the second term is called Paulian, since Pauli [6] showed that in describing particles having spin 1/2 the conventional Dirac equation

$$\left(\gamma_\lambda \frac{\partial}{\partial x_\lambda} + M - ie\gamma_\lambda A_\lambda\right)\Psi = 0 \qquad (\hbar = c = 1),$$

which considers the interaction with an electromagnetic field (the term $-ie\gamma_\lambda A_\lambda$), may have the term $(ie\varkappa/2M)\gamma_\lambda\gamma_\nu F_{\lambda\nu}$ added to it, where $F_{\lambda\nu}$ is the electromagnetic-field tensor, while $\varkappa$ is a certain arbitrary constant which may be interpreted as the additional nucleon magnetic moment. For a transfer t → 0 the second term can be normalized as follows:

$$i\langle \bar{w}(p') | (F_2^s(0) + F_2^v(0)\tau_3)\sigma_{\lambda\nu}k_\nu | w(p)\rangle = i\frac{e}{2M}\langle \bar{w}(p') | (\varkappa_s + \varkappa_v\tau_3)\sigma_{\lambda\nu}k_\nu | w(p)\rangle,$$

whence it follows for a proton

$$F_{2p}(0)=F_2^s(0)+F_2^v(0)=\frac{e}{2M}(\varkappa_s+\varkappa_v)=\frac{e}{2M}\varkappa_p,$$

while for a neutron

$$F_{2n}(0)=F_2^s(0)-F_2^v(0)=\frac{e}{2M}(\varkappa_s-\varkappa_v)=\frac{e}{2M}\mu_n.$$

Since the anomalous proton magnetic moment $\varkappa_p = 1.79$, while the anomalous neutron magnetic moment $\varkappa_n$ (it is the total neutron magnetic moment $\mu_n$) is given by $\varkappa_n = \mu_n = -1.91$, it follows that

$$F_2^s=\frac{e}{2M}\cdot\frac{\varkappa_p+\varkappa_n}{2}=-0.06\frac{e}{2M};$$

$$F_2^v=\frac{e}{2M}\cdot\frac{\varkappa_p-\varkappa_n}{2}=1.85\frac{e}{2M}.$$

From this it is evident that the principal contribution to the proton and neutron form factors $F_2(q^2)$ is made by the isotopic vector part.

The two $\pi$-meson and nucleon vertices displayed above may be treated as parts of Feynman graphs describing the scattering processes

$$e+\pi\to e+\pi; \tag{4a}$$

$$e+N\to e+N. \tag{4b}$$

In the general case the total collection of relativistic structural coefficients for the scattering amplitudes (4) turns out to be larger than the number of form factors considered above. This is associated with the fact that the total amplitude of the scattering processes (4) includes an infinitely large collection of diagrams in addition to the diagrams displayed in Figs. 3 and 6; this collection includes, for example, exchange of two, three, etc., photons, which in general leads to an increase in the number of invariant functions or, stated differently, an increase in the number of relativistic structural coefficients. The total number of relativistic structural coefficients is determined by the number of free ends on the Feynman diagram and the presence of spins and isotopic spins of the particles described by the free ends. In the case of a finite number of free ends on the Feynman diagram, the number of structural coefficients will be finite. For amplitudes of the type

$$a+b\to c+d$$

the number of relativistic structural coefficients M (the isotopic structure of the amplitudes is not considered here) can be determined by the following formulas [7].

1. If the spins of all particles participating in the reaction are integer spins, then

$$M=\frac{1}{2}[(2i_a+1)(2i_b+1)(2i_c+1)(2i_d+1)+\beta(-1)^{i_a+i_b+i_c+i_d}],$$

where $i_a$ is the spin of particle $a$; $\beta=\frac{\chi_a\chi_b}{\chi_c\chi_d}$, $\chi_a$ is the internal parity of particle $a$.

2. In all remaining cases

$$M=\frac{1}{2}(2i_a+1)(2i_b+1)(2i_c+1)(2i_d+1).$$

The isotopic structure of the processes considered can easily be sought by means of the rule for the addition of isotopic particle spins and the isotopic spin conservation laws. For elastic-scattering processes $a + b \to a + b$ invariance relative to time inversion reduces the number of structures. In particular, for the $e + N \to e + N$ process the number of relativistic structural coefficients decreases from eight to six. With allowance for istopic invariance, the number of structural coefficients in these reactions increases to 12.

The vertex parts displayed in Figs. 3 and 6 may also be treated as parts of Feynman graphs which describe annihilation processes:

$$e^- + e^+ \to \pi^- + \pi^+; \tag{5a}$$

$$e^- + e^+ \to N + \tilde{N}. \tag{5b}$$

In this case the expressions for the vertex parts will have the form:

$$\left.\begin{aligned}
&\langle 0 \mid j_\lambda \mid \pi\tilde{\pi}\rangle = \frac{(\pi^+ - \pi^-)_\lambda}{\sqrt{4\omega_+\omega_-}} F_\pi(t),\\
&t = (\pi^+ + \pi^-)^2 \geqslant 4m_\pi^2,\\
&\langle 0 \mid j_\lambda^N \mid N\tilde{N}\rangle = \frac{1}{\sqrt{4E_N E_{\tilde{N}}}} \langle \bar{w}_{\tilde{N}}(p_{\tilde{N}}) \mid (F_1^s(t) + F_1^v(t)\tau_3)\gamma_\lambda +\\
&\qquad + i(F_2^s(t) + F_2^v(t)\tau_3)\sigma_{\lambda\nu}k_\nu \mid w_N(p_N)\rangle,\\
&t = (p_{\tilde{N}} + p_N)^2 \geqslant 4M^2.
\end{aligned}\right\} \tag{6}$$

Here the form-factor function of $\pi$-mesons and nucleons differ from those written out previously in (3) in their range of variation of the variable t.

In field theory it is stated that the form-factor function $F_\pi(t)$ must be the same function for both the scattering process (4a) and the annihilation process (5a). A similar statement is also made with regard to the form-factor functions of nucleons. The dispersion relations ensure the necessary link between form-factor functions stipulated in various t-domains.

## 2. THE ELECTROMAGNETIC FORM FACTOR OF A $\pi$-MESON

An investigation of the analytic properties of the vertex function of a $\pi$-meson [8, 2] leads to the statement that $F_\pi(t)$ is an analytic function in the t plane having a cut $4m_\pi^2 \leqslant t \leqslant \infty$, i.e., for the $e^+ + e^- \to \pi^+ + \pi^-$ annihilation process the form factor of the $\pi$-meson is a complex quantity, whereas in the domain $t < 0$ (i.e., for the $e + \pi \to e + \pi$ scattering process) $\mathrm{Im}\, F_\pi(t) = 0$ and the form factor is a real quantity. Thus, the dispersion relation has the form

$$F_\pi(t) = \frac{1}{\pi}\int_C \frac{\mathrm{Im}\, F_\pi(t')\, dt'}{t' - (t + i\varepsilon)}. \tag{7}$$

The integration contour is depicted in Fig. 7. The imaginary correction $i\varepsilon$ to the value of t denotes that the form factor $F_\pi(t)$ takes observable values as it approaches the real axis from above. In the subsequent exposition the imaginary corrections $i\varepsilon$ will be dropped throughout. Performing the transition in the limit in the denominator of the integrand expression (7), we obtain*

$$\mathrm{Re}\, F_\pi(t) = \frac{\mathcal{P}}{\pi}\int_C \frac{\mathrm{Im}\, F_\pi(t')}{t' - t}\, dt'. \tag{7a}$$

*The symbolic equation

$$\frac{1}{t' - (t \pm i\varepsilon)} = \frac{\mathcal{P}}{t' - t} \pm i\pi\delta(t' - t).$$

is used.

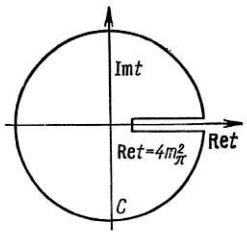


Fig. 7. Integration contour in the complex plane of the variable t.

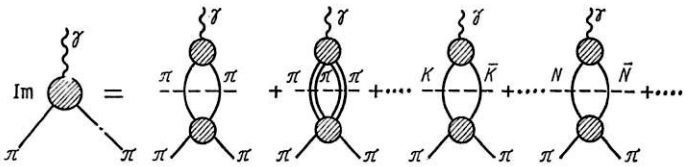


Fig. 8. Graphical representation of the unitarity condition.

The behavior of $\mathrm{Im}\,F_\pi(t)$ for $t \to \infty$ is unknown. But if it is assumed that $\lim_{t\to\infty} \mathrm{Im}\,F_\pi(t) = \mathrm{const}$, then it follows that for convergence of the integral (7) it is required to carry out one deduction. We shall carry out the subtraction at the point t = 0, where $F_\pi(0) = e$. Then the dispersion relation has the form

$$F_\pi(t) - F_\pi(0) = \frac{t}{\pi} \int_{4m_\pi^2}^{\infty} \frac{\mathrm{Im}\,F_\pi(t')\,dt'}{t'(t'-t)}. \tag{8}$$

Relationship (8) is still an identity and may not be used for applications. In order to convert it into an equation it is necessary to make use of additional information. Further work on calculating the function $F_\pi(t)$ depends on the assumptions concerning the behavior of $\mathrm{Im}\,F_\pi(t)$ in the domain $t \geq 4m_\pi^2$. For this purpose we use the unitarity condition

$$\mathrm{Im}\,\langle 0|j_\nu|\pi^+\pi^-\rangle = \sum_\alpha \langle 0|j_\nu|\alpha\rangle\langle\alpha|T^+|\pi^+\pi^-\rangle, \tag{9}$$

where $T^+$ denotes the Hermite-conjugate amplitude, while $\alpha$ takes all states allowed by the conservation laws (in particular, states with a total angular momentum J = 1, since a photon has a spin equal to 1). The lowest state is the state having two $\pi$-mesons; the $3\pi$-state is forbidden, since $\langle\alpha|T^+|\pi^+\pi^-\rangle = 0$ according to a theorem similar to the Furry theorem in electrodynamics. The next allowed state is the $\alpha$-state with four $\pi$-mesons, etc. Among the $\alpha$ states $K\bar{K}$, $N\bar{N}$, NN, $\pi\pi$, etc., pairs are possible. Their production threshold with respect to t lies far from the beginning of the cut, which is frequently used in specific calculations.

Equation (9) is displayed graphically in Fig. 8. Here it is appropriate to recall that the dispersion relations (7) or (8) together with the unitarity condition (9) in principle provide the possibility of carrying out the summation of an infinitely large number of the diagrams displayed in Fig. 3 or Fig. 6. For this purpose it is necessary to write out the dispersion relations for all amplitudes which are included in the unitarity condition (9) and to solve the infinite system of nonlinear singular integral equations. It is clear that this problem is unsolvable, and in practical calculations the practice is to restrict the analysis to the simplest cases.

Assume that we are interested in the region of small values of t. Whereas now there are no states in the unitarity condition for $t' > t$ which make anomalously large contributions, then the high-energy region will yield a small contribution which differs little from a constant, since the denominator of the integrand Eq. (8) may be written in the form

$$t'(t'-t) = t'^2\left(1 - \frac{t}{t'}\right) \approx t'^2.$$

Thus, under the assumptions considered one may limit the analysis to the lowest states from $\alpha$. In the consideration given let us limit ourselves to one state from $\alpha$ – the $2\pi$-meson state. Then condition (9) takes the form

$$\mathrm{Im}\,\langle 0|j_\lambda|\pi\pi\rangle \approx \langle 0|j_\lambda|\pi\pi\rangle\langle\pi\pi|T^+|\pi\pi\rangle.$$

The vertex $\langle 0|j_\lambda|\pi\pi\rangle$ can be described by one p-wave. Therefore, the amplitude $\langle\pi\pi|T^+|\pi\pi\rangle$ must likewise be described by one p-wave. Starting from the given parity condition for the matrix S, we obtain the following expression for the imaginary part of the form factor:

$$\operatorname{Im} F_\pi(t) = F_\pi(t)\, e^{-i\delta_1(t)} \sin\delta_1(t) \tag{10}$$

where

$$\operatorname{Im} F_\pi(t) = \operatorname{Re} F_\pi(t) \operatorname{tg}\delta_1(t), \tag{11}$$

and $\delta_1(t)$ is the phase of the $\pi\pi$-interaction corresponding to the quantum numbers I = 1, J = 1. Having substituted (11) into Eq. (8), we obtain

$$\operatorname{Re} F_\pi(t) = e + \frac{t}{\pi} \mathcal{P} \int_{4m_\pi^2}^{\infty} \frac{\operatorname{Re} F_\pi(t') \operatorname{tg}\delta_1(t')}{t'(t'-t)}\, dt'. \tag{12}$$

Thus, the form-factor functions satisfy a linear singular integral equation which may be solved by the Muskhelishvili-Omnes method [9]. The general solution of Eq. (12) has a somewhat cumbersome form. Therefore, for simplicity we write out the solution of the integral equation without subtraction:

$$F_\pi(t) = e \exp\left\{\frac{t}{\pi} \mathcal{P} \int_{4m_\pi^2}^{\infty} \frac{\delta_1(t')\, dt'}{t'(t'-t)}\right\}. \tag{13}$$

Making various assumptions concerning the character of the behavior of the $\delta_1$-phase of $\pi\pi$-scattering, one can obtain various expressions for $F_\pi(t)$. The integration in (13) may be carried to completion by means of the theory of residues if the behavior of the phase $\delta_1$ is chosen to be in the form of the ratio of polynomials P(k) and Q(k) [10]:

$$k^3 \operatorname{ctg}\delta_1(t) = \frac{P(k)}{Q(k)},$$

where k is the three-dimensional momentum of a $\pi$-meson in a coordinate system in which a pair of $\pi$-mesons is produced. The invariant variable in this coordinate system is equal to the square of the total energy of two $\pi$-mesons: $t = 4(k^2 + 1)$; $m_\pi = 1$.

For the scattering of an electron by a $\pi$-meson in the center of mass system in the case of back scattering the invariant variable t has the form

$$t = -2\nu(1 - \cos 180^\circ) = -4\nu = -4(\omega^2 - 1), \quad \omega = ik.$$

After integrating the relationship (13) we obtain

$$F_\pi(\nu) = e \prod \frac{i\omega - k_j}{i\omega + k_i} \cdot \frac{i + k_i}{i - k_j}, \quad \operatorname{Im} k_i > 0, \quad \operatorname{Im} k_j < 0,$$

where $k_{i,j}$ are the roots of the equations $1 + i \operatorname{tg}\delta_1 = 0$, $\nu = \omega^2 - 1$. For $\nu = 0$ the energy $\omega = 1$ and $F_\pi(0) = e$. In particular, choosing the behavior of the phase $\delta_1$ to be of the form $ak^3 \operatorname{ctg}\delta_1(k) = k_r^2 - k^2$, which correspond to the choice of the resonance Breit-Wigner equation

$$e^{i\delta_1} \sin\delta_1 = \frac{ak^3}{k_r^2 - k^2 - iak^3} \tag{14}$$

and assuming $\varepsilon = ak_r < 1$, we obtain

$$F_\pi(\nu) = e \frac{k_r + \dfrac{1}{\varepsilon + k_r}}{k_r + \dfrac{\omega^2}{\varepsilon\omega + k_r}}. \tag{15}$$

If in Eq. (15) we carry out the expansion of the expression $1/(\varepsilon\omega + k_r)$ for the condition $\varepsilon\omega/k_r < 1$, then the form factor (15) goes over into the expression

$$F_\pi(t) = e\frac{t_r - 4a}{t_r - t - 4iak^3} \tag{16}$$

and coincides with the form factor obtained in [11] for a $\pi$-meson. At the point t = 0 the quantity k = i, and F(0) = e.*

The form factor (15) enters into the dispersion relation for the scattering of $\pi$-mesons by nucleons. Resonance interaction of $\rho$-mesons taken in the form (14) can be explained as exchange of a $\rho$-meson ($\pi + \pi \to \rho \to \pi + \pi$), whose mass is equal to $m_\rho$ = 750 MeV. For a value of the parameter $\varepsilon = 0.2$, one can provide a good explanation of the experimental data on the scattering of $\pi$-mesons by nucleons [10], which justifies the approximations used in the derivation of Eq. (15).

An original approach to a description of the electromagnetic form factor of a $\pi$-meson was proposed in [12, 13]. Its essence resides in the fact that the dispersion relations for the form-factor function includes integrals within finite limits over that range of momentum transfers in which experimental data is available. The problem consists in finding the form-factor function of a $\pi$-meson and determining the boundary of the variation $r_\pi$ of the electromagnetic radius of a $\pi$-meson. In particular, in [13] the author was able to obtain agreement between the experimental data and the analytic properties of a $\pi$-meson form factor and to estimate the upper boundary of the value $r_\pi < 0.8$ F.

An example of the nondispersive approach to a description of the form factor of $\pi$-meson may be found in [14]. The author uses the hypothesis of minimality of the electromagnetic interaction

$$i\partial_\mu J_\mu^Q(x) = QeA_\mu(x) J_\mu^Q(x),$$

where Q = +, −, 0; $J_\mu^Q$ is the current which considers strong and electromagnetic interactions; $A_\mu$ is the electromagnetic potential. In the absence of electromagnetic interaction the theory of strong interactions is isotopically invariant, and then the right side of the equation is equal to zero. The interaction which appears in the right side of the expression leads to electromagnetic splitting of the masses of the isotopic multiplet (in the case given this multiplet is a $\pi$-meson triplet). If from this interaction we take the matrix element between one-pion states, then it can be seen that in the $e^2$-approximation it turns out to be linked to the electromagnetic form factor of a $\pi$-meson:

$$\langle \pi_2 s' | J_\mu^Q | \pi_1 s\rangle = \frac{(\pi_1 + \pi_2)_\mu}{\sqrt{4\omega_1\omega_2}} F_\pi(\pi_2\pi_1) T_{ss'}^Q + i\alpha | Q | T_{ss'}^Q (\pi_1 - \pi_2)_\mu G(\pi_2\pi_1),$$

where $T_{ss'}^Q$ are the isotopic matrices of the triplet; $\alpha$ is the fine-structure constant; $F_\pi(\pi_2\pi_1)$ is the form-factor function of a $\pi$-meson; $G(\pi_2\pi_1)$ is a function which is linked with the radiation correction to $\beta$-decay of a $\pi$-meson; s is the isotopic index of a $\pi$-meson. The form-factor function $F_\pi(\pi_2\pi_1)$ satisfies the equation

$$F_\pi(\pi_2\pi_1) = \frac{\alpha}{32\pi^2 m_\pi \Delta m_\pi} \int \frac{d^3q}{\omega} \cdot \frac{(\pi_1 + q)_\mu (\pi_2 + q)_\mu}{\pi_2 q - m_\pi^2} F(\pi_2 q) F(q\pi_1)$$

with the additional condition $F_\pi(m_\pi^2) = 1$.

In deriving this equation the one-particle approximation was used in the expansion of the product of the currents in the full collection of functions. This led to a situation in which it contained only one integral

*Having placed the value of $a$ equal to zero and e = 1 in Eq. (16), we obtain the conventional expression for the form factor of a $\pi$-meson in the pole approximation (a $\rho$-pole):

$$F_\pi(t) = \frac{1}{1 - \frac{t}{t_\rho}} \qquad \text{[see Eq. (17a)].}$$

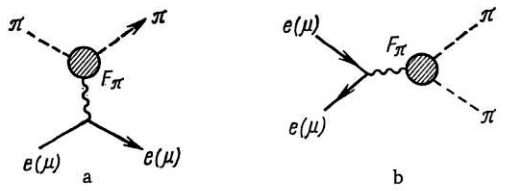


Fig. 9

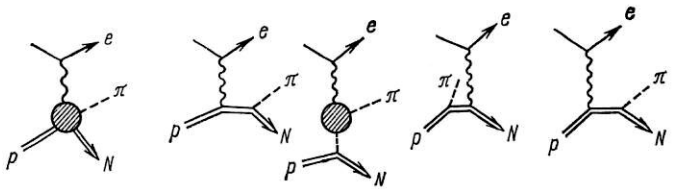


Fig. 10

Fig. 9. Process of electron ($\mu$-meson) scattering by $\pi$-mesons (a) and annihilation of electrons and positrons ($\mu\pm$-mesons) into a pair of $\pi$-mesons, in which the electromagnetic form factor of a $\pi$-meson is measured (b).

Fig. 10. The various contributions to the amplitude of $\pi$-meson electroproduction.

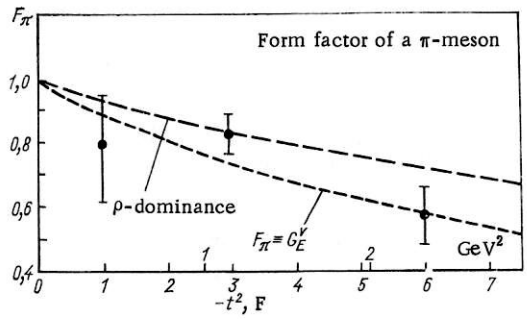


Fig. 11. Comparison of the experimental data with theoretical curves.

term and was a nonlinear integral equation. Consideration of the other states would lead to the addition of other integral terms of the type

$$\int \frac{\prod_n d^3q_n}{\omega_n} \ldots \Phi(\pi_2 q_1 \ldots q_n)\,\Phi(q_1 \ldots q_n \pi_1),$$

in the right side of the equation considered; these terms contain products of more complex vertex functions which depend on many variables instead of the product of form-factor functions $F(\pi_2 q)\ F(q\pi_1)$. It is very difficult to estimate the correction of the approximation used by the author. For the equation considered the approximate analytic solution is sought by expansion into a series in eigenfunction of the motion group in Lobachevskii space in the domain of small momentum transfers. In this case the solution is simply related to the mean-square electromagnetic radius (see Eq. (2)). The approximate solutions found in this manner have the form

$$F(q^2) = \left[1 - \frac{q^2}{6}\left(\frac{\varepsilon}{1-2\varepsilon} + 16\varepsilon^2\right) + \ldots\right] e,$$

where $\varepsilon = \alpha m_\pi / 8\Delta m_\pi$; $\alpha = 1/137$; $m_\pi = 135$ MeV; $\Delta m = 4.6$ MeV. The substitution of numerical values leads to the value $\langle r \rangle = 0.23\ m_\pi^{-1} \approx 0.3$ F.

The form factor of a $\pi$-meson can be measured experimentally in all reactions which contain a vertex $\gamma \to 2\pi$. However, obtaining experimental data on the form factor of a $\pi$-meson is an exceptionally difficult matter. Usually a number of other quantities which are determined from the same experiment is included in the investigated processes besides the form factor of a $\pi$-meson. This complicates an unambiguous isolation of the form-factor function. Only in scattering of electrons or $\mu$-mesons by $\pi$-mesons (Fig. 9a) or in the $e + e \to \pi + \pi$, $\mu + \mu \to \pi + \pi$ (Fig. 9b) can one measure the form factor of a $\pi$-meson in the most efficient manner.

The $\pi + e \to \pi + e$ process was studied for the scattering of $\pi$-mesons by the electrons of various nuclei (see, for example, [15]). However, for low $\pi$-meson energies the electron recoil is small, in connection with which high requirements develop governing the accuracy of the experiment on the one hand, while on the other hand the form-factor function $F_\pi(t)$ is determined in a small domain of space-like momentum transfers in which $F_\pi(t)$ differs little from unity.

In [16] the form factor of a $\pi$-meson in the domain of space-like transfers was measured during the process of the electrical production of a $\pi$-meson (Fig. 10):

$$e + p \to e + N + \pi.$$

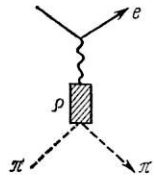


Fig. 12

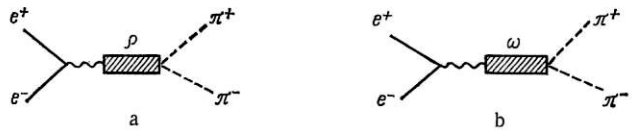


Fig. 13

Fig. 12. Feynman diagrams describing e + π → + e + π scattering in the ρ-dominant approximation.

Fig. 13. Sum of the contributions to the form factor $F_\pi$: *a*) ρ-exchange diagram with allowance for $\Gamma_\rho$; b) diagram which considers the contribution of the interference $\rho - \omega$ term.

The experimental points have rather large errors which are generated not only by the experimental errors but also by the estimates of the reality of the theoretical description. Figure 11 gives a comparison of experimental data (the points) with two theoretical curves

$$F_\pi(t) = \frac{1}{1 - \frac{t}{m_\rho^2}} \tag{17a}$$

(ρ is the dominant model, see Fig. 12);

$$F_\pi(t) \equiv G_E^v, \tag{17b}$$

where $G_E^V$ is the isotopic vector part of the electrical nucleon form factor (see § 6 of the present review).

Equation (17a) derives trivially from Eq. (17) if instead of the imaginary part $\mathrm{Im}F_\pi(t)$ we substitute the expression $\pi g_{\rho\gamma} g_{\pi\pi\rho} \delta(t - m_\rho^2)$ (i.e., if we choose $\mathrm{Im}F_\pi(t)$ in the pole approximation having a zero decay width).* The quantities $g_{\rho\gamma}$ and $g_{\pi\pi\rho}$ are the coupling constants of a ρ-meson with a γ-quantum (see Fig. 1c) and of a ρ-meson with π-mesons, respectively. If in the ρ-dominant approximation the value of $m_\rho$ is chosen to equal (600 ± 80) MeV, then the average value of the electromagnetic radius of a π-meson $r_\pi$ [the determination of $r_\pi$ is given in Eq. (2)] turns out to equal (0.80 ± 0.10) F.

With the launching of the Serpukhov accelerator (The Institute of High-Energy Physics) it will be possible to obtain beams of π-mesons having a momentum $\gtrsim 50$ MeV/c which will ensure the investigation of the form factor of a π-meson up to transfers of $q = \sqrt{-t} \gtrsim 200$ MeV/c. Under these conditions the mean-square radius $\sqrt{\langle r \rangle^2} \approx 0.7$ F can be measured with an error which is as small as 0.1 F [17]. The correct estimation of the radiation corrections is of important significance.

In [18] the radiation corrections to the process of elastic π − e scattering were calculated in a kinematics that maximally approximates the kinematics of the experiment planned [17] at the Joint Institute for Nuclear Research, which will be carried out at Serpukhov (Institute of High-Energy Physics). Before [18] the radiation corrections to scattering were calculated in the Kahane paper [19] for the case when the energies of the scattered particles are measured. However, in order to isolate the background processes, the

*In the domain t < 0 we have $F_\pi(t) = \mathrm{Re}\, F_\pi(t)$. In Eq. (7a) the denominator $t' - t \neq 0$ for $t < 0$, and therefore the symbol $\mathcal{P}$ may be dropped:

$$\mathrm{Re}\, F_\pi(t) = F_\pi(t) = \frac{1}{\pi} \int \frac{\pi g_{\pi\gamma} g_{\pi\pi\rho} \delta(t' - m_\rho^2)\, dt'}{t' - t} = \frac{g_{\pi\gamma} g_{\pi\pi\rho}}{t_\rho - t};\ t_\rho = m_\rho^2.$$

The quantity $\frac{g_{\rho\gamma} g_{\pi\pi\rho}}{m_\rho^2} \approx 1$. From this we obtain Eq. (17a) for the form factor of a π-meson which is normalized to unity F(0) = 1 rather than to the charge e.

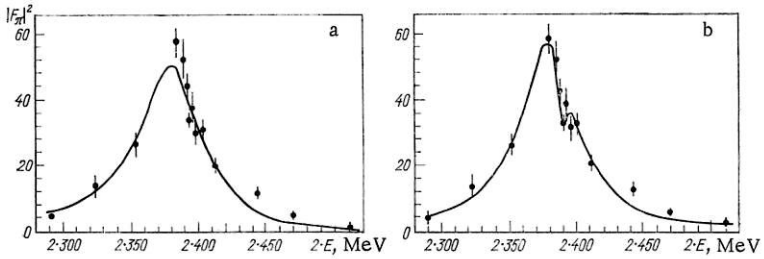


Fig. 14. Comparison of theoretical calculations with experimental data for $\xi = 0$ (a) and $\xi = \xi(E, \alpha) \neq 0$ (b) [23].

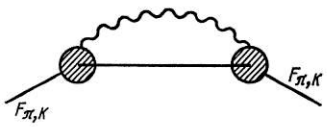


Fig. 15. Electromagnetic correction to the meson mass in the lowest order of perturbation theory.

planned experiments will measure the energies and emission angles of the final particles and also verify the coplanarity of the momenta. It is obvious that the measurements of additional parameters will affect the magnitude of the radiation corrections. In [18] the radiation corrections were calculated for the case of measuring three parameters (the energies of the final particles and the emission angle of the scattered $\pi$-meson) out of the five enumerated above. The conditions and ranges of variation of the measured parameters within which the additional measurement of the two remaining parameters does not alter the magnitude of the radiation corrections were indicated. An analysis is carried out of the contribution of the $\rho$-mesons in the diagram of two-photon exchange.

Recently the form factor of a $\pi$-meson was investigated in the domain of time-like transfers $t > 0$, (i.e., in the $e^+ + e^- \to \pi^+ + \pi^-$ process) in a number of papers [20-23]. It can easily be seen (see Fig. 9b) that the cross section of the process will be proportional to the square of the modulus of the form factor $F_\pi$. In [23] values of $|F_\pi|^2$ were obtained in the following range of energies E:

$$300 \leqslant E \leqslant 500 \text{ MeV},$$

where E is the energy of an electron (or positron in the center of mass system of the reaction $e^+ + e^- \to \pi^+ + \pi^-$).

It is assumed that the principal contribution to $F_\pi$ is made by the $\rho$-exchange diagram (Fig. 13a) with allowance for the width $\Gamma_\rho$ of $\rho$-meson decay. In order to consider the possible contribution of the interference $\rho - \omega$ terms, a diagram (Fig. 13b) with the multiplier $\xi e^{i\alpha}$ is added to the diagram shown in Fig. 13a. The full expression for the form factor $F_\pi$ is written in the form

$$F_\pi(s) = \frac{m_\rho^2\left(1+\frac{\Gamma_\rho}{m_\rho}d\right)}{m_\rho^2 - 4E^2 + im_\rho\Gamma_\rho\left(\frac{p}{p_0}\right)^3\frac{m_\rho}{2E}} + \xi e^{i\alpha}\frac{m_\omega^2}{m_\omega^2 - 4E^2 + im_\omega\Gamma_\omega}, \tag{18}$$

where $\xi$ and $\alpha$ are free parameters which describe the $\rho - \omega$ interference, and d is chosen in such a way that the $\rho$-meson part of the form factor is normalized to unity for zero momentum transfer (d = 0.48); $p = \sqrt{E^2 - m_\pi^2}$; $p_0 = \sqrt{\frac{m_\rho^2}{4} - m_\pi^2}$, $s = 4E^2$. The results of comparing the theoretical calculations with the experimental data are displayed in Fig. 14. From this comparison it is evident that the case $\xi \neq 0$ is preferable, although the case $\xi = 0$ cannot be excluded entirely.

## 3. THE ELECTROMAGNETIC MASS DIFFERENCE AND FORM FACTORS OF K-MESONS [24]

The problems of the theoretical explanation of the observed mass difference and calculating the form factors of K-mesons are interrelated. This link depends on the assumptions made concerning strong interactions of K-mesons with other particles.

Independently of these assumptions a general formula relating the electromagnetic correction to the mass of a particle having a virtual Compton-effect amplitude $T_{\mu\nu}$ (see Fig. 5) is valid:

$$\Delta m = \frac{1}{8\pi^2} \int \frac{T_{\mu\nu}(q^2, \nu)\, g^{\mu\nu}}{q^2 + i\varepsilon} d^4q, \tag{19}$$

where $\nu = pq/m$; q is the photon momentum; p is the particle momentum.

Riazzudin [25], restricting itself to the one-meson contribution to the imaginary part of the amplitude of photon scattering by mesons, obtained an approximate equation for the corrections of the mass corresponding to the diagram displayed in Fig. 15:

$$\Delta m^2 = \frac{i\alpha}{4\pi^3} \int \frac{d^4q}{q^2 + i\varepsilon} F_\pi^2(q^2) \left[2 + \frac{q^2 - 4m^2}{q^2 - 2pq}\right]. \tag{20}$$

If one uses a pole approximation of the type of Eq. (17a) for the form factor of a $\pi$-meson, then Eq. (20) may be used to obtain the correct mass difference for $\pi$-mesons, but the pole approximation for the form factors of K-mesons and Eq. (20) yield the incorrect sign of the mass difference for K-mesons (instead of $\delta m_K = m_{K^+} - m_{K^0} = -4$ MeV the theory yields a positive value of $\delta m_K$).

There are two ways of affecting the calculations:

1) to reject Eq. (20) and go over to Eq. (19) with a more exact approximation of the amplitude $T_{\mu\nu}$ and

2) to modify the form factor $F(q^2)$ on the assumption that Eq. (20) is fairly accurate.

Tanaka [26], having chosen the first way, considered the contributions from the K*- and $K_A$-resonance states in the amplitude of the virtual Compton-effect involving K-mesons. The terms which develop under these conditions in the expressions for the mass difference contain diverging integrals. The truncation constant must be chosen fairly far out; however, one can obtain the required mass difference. An unsuccessful choice of the truncation constant is evidently associated with the fact that a good asymptotic behavior has not been found for the amplitude.

G. Zinov'ev and B. Struminskii [27] obtained the correct difference of the K-meson masses after having improved the consideration of the asymptotic behavior of the amplitude $T_{\mu\nu}$ of the virtual Compton-effect in Eq. (19). They assumed that the amplitude $T_{\mu\nu}$ has a Regge asymptotic behavior $\sim \nu^{\alpha(0)}$ which is determined by the $A_2$-meson. The Regge residue $\beta(q^2)$ associated with the $A_2$-meson was found by the authors using the sum rules for the final energy. The value of the Regge residue depends on the value of the coupling constant $g^2_{K^*K\gamma}$ of the decay $K^* \to K\gamma$. This constant was determined from the decay $\omega \to \pi\gamma$ using SU(3)-symmetry.

Thus, the first way—rejection of Eq. (20) and refinement of the form $T_{\mu\nu}(q^2, \nu)$—leads to the correct value of the difference $\delta m_K$.

The second way—modification of the form factor $F_K(q^2)$—may likewise lead to a positive result.

Ogievetskii and Chou Huan-Chao [28] derived the correct expression for the mass difference using Eq. (20) and K-meson form factors of the form:

$$\left.\begin{aligned} F_K^v &= \frac{(4m_K^2)^2}{(4m_K^2 - q^2)^2}(1 - \lambda) + \lambda \frac{4m_K^2}{4m_K^2 - q^2}; \\ F_K^s &= \frac{(4m_K^2)^2}{(4m_K^2 - q^2)^2}(1 + \lambda) - \lambda \frac{4m_K^2}{4m_K^2 - q^2}, \end{aligned}\right\} \tag{21}$$

where $\lambda$ is the parameter; $\lambda = 2$. The form factors (21) have correct normalization, but the presence of double poles, the positions of the poles, and the residues at them regrettably have no physical substantiation.

One may attempt to find form factors $F_K^{V,S}$ having a more natural behavior at low energies:

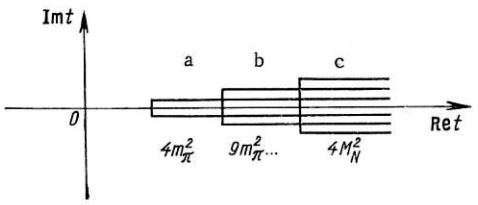


Fig. 16. The beginning of the cuts in the unitarity condition (24) for states $\alpha$ containing two $\pi$-mesons (a), three $\pi$-mesons (b), and a nucleon-antinucleon pair (c).

a) the form factor $F_K^V$ must have a pole corresponding to a $\rho$-meson;

b) the form factor $F_K^S$ must have poles corresponding to $\omega$- and $\varphi$-mesons;

c) $F_K^V$ must be related by the two-particle unitarity condition to the amplitude of the $\pi\pi \to K\bar{K}$ process. An amplitude calculated according to the Venezziano model is chosen as the amplitude of $\pi\pi \to K\bar{K}$;

d) the form factors must have the correct normalization;

e) for describing the integral contribution of the high-energy domain one may use the parametrization $aS^{-b}$ which reminds one of the behavior of Regge amplitudes. The principal conclusion which is obtained from assumptions a–e) is the following: the difference $\delta m = m_{K^+} - m_{K^0} = -4$ MeV can be obtained using the modified form factor $F_K^V$:

$$F_K^v = \frac{1}{1-\frac{t}{m_\rho^2}} - C\int_{s_0}^{\infty} \frac{ds'}{s'\ s}\left(\frac{s'}{m_\rho^2}\right)^{-b}, \tag{22}$$

where C, b, and $s_0$ are arbitrary parameters.

The form factor $F_K^V$ at low energies can be described well by the pole approximation, while at high energies it has a slowly decreasing "tail." The quantity b may be small $(10^{-3} \leqslant b \leqslant 10^{-2}); 10^{-5} \leqslant C \leqslant 10^{-2}$, $s_0$ is an arbitrary parameter beginning with which the contribution of the high-energy domain is considered; the dependence on the choice of $s_0$ is weak.

## 4. DESCRIPTION OF NUCLEON FORM FACTORS BY MEANS OF DISPERSION RELATIONS

The dispersion relations for nucleon form factors are written by complete analogy with the dispersion relations for the $\pi$-meson form factor. Let us agree to start by writing the dispersion relations for the isotopic form factors (the scalar $F^S$ and vector $F^V$ form factors) having one deduction:

$$F_{1,2}^v(t) = F_{1,2}^v(0) + \frac{t}{\pi}\int_{4m_\pi^2}^{\infty} \frac{\operatorname{Im} F_{1,2}^v(t')\,dt'}{t'(t'-t)}; \tag{23a}$$

$$F_{1,2}^s(t) = F_{1,2}^s(0) + \frac{t}{\pi}\int_{9m_\pi^2}^{\infty} \frac{\operatorname{Im} F_{1,2}^s(t')\,dt'}{t'(t'-t)}. \tag{23b}$$

In the last section of the review we shall consider dispersion relations with no deductions.

The imaginary parts $\operatorname{Im} F_{1,2}^{V,S}$ for the nucleon current (6) are found from the unitarity condition for the S-matrix (S = 1 + i T):

$$\operatorname{Im}\langle 0|j_\lambda^{s,v}|N\bar{N}\rangle = \sum_\alpha \langle 0|j_\lambda^{s,v}|\alpha\rangle\langle\alpha|T^+|N\bar{N}\rangle. \tag{24}$$

The physical threshold of the process considered begins with an energy $t \geq 4M^2$. However, the intermediate states $\alpha$ may contain a $2\pi$-meson, a $3\pi$-meson, and an infinite set of other states (Fig. 16). For a number of low intermediate states the quantities $\operatorname{Im} F_{1,2}^{S,V}$ turn out to be nonvanishing in the nonphysical domain $t \lesssim 4M^2$. From an analysis of Eq. (24) it follows (see, for example, [2]) that the isovector functions $\operatorname{Im} F_{1,2}^V$ are nonvanishing in the domain $t \geq 4m_\pi^2$ and a contribution to them is made only by the states $\alpha$ having an

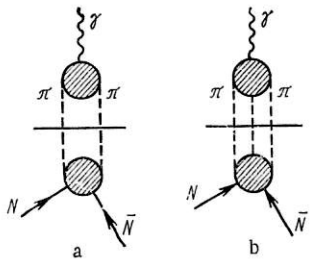


Fig. 17. Graphical representation of the unitarity condition.

even number of $\pi$-mesons, while the isoscalar functions $\mathrm{Im}F^{S}_{1,2}$ are non-vanishing in the domain $t \geq 9\ m_\pi^2$ and a contribution to them is made only by the states $\alpha$ having an odd number of $\pi$-mesons. This can explain the different lower limits in Eqs. (23a) and (23b). The use of double Mandel'shtam dispersion relations allows us to obtain the analytic continuation of the unitarity condition from the physical domain $t \geq 4\ M^2$ into the domain of non-physical values $4m_\pi^2 \leq t \leq 4M^2$. Therefore, there are no difficulties in principle in carrying out the theoretical calculations. Let us proceed further by analogy with the procedure used in describing the form factor of a $\pi$-meson. For low values of t we retain only one lowest intermediate state each in the unitarity condition (24) on the assumption that all of the remaining higher intermediate states make a negligibly small contribution. This means that for the isovector form factors only the $2\pi$-meson intermediate state remains, and the expressions for the function $\mathrm{Im}F^{V}_{1,2}$ take the form

$$\mathrm{Im}\,F^{v}_{1,2} = F_\pi(t)\,\langle \pi\pi\,|\,T^{+}_{1,2}\,|\,N\tilde{N}\rangle, \tag{25}$$

where $F_\pi(t)$ is the form factor of a $\pi$-meson, while $\langle \pi\pi\,|\,T^{+}\,|\,N\tilde{N}\rangle$ are the parts of the amplitude of the annihilation process $\pi\pi \to N\bar{N}$, which make contributions to the Dirac or Pauli form factors, respectively. And for the imaginary parts of the isoscalar form factors only the three-meson intermediate state remains, and the expressions for them can be represented in the form of a product of two amplitudes:

$$\mathrm{Im}\,F^{s}_{1,2}(t) = \langle \gamma\,|\,T\,|\,\pi\pi\pi\rangle\,\langle \pi\pi\pi\,|\,T^{+}_{1,2}\,|\,N\tilde{N}\rangle, \tag{26}$$

where $\langle \gamma\,|\,T\,|\,\pi\pi\pi\rangle$ is the $\gamma \to 3\pi$ vertex, while $\langle \pi\pi\pi\,|\,T^{+}_{1,2}\,|\,N\tilde{N}\rangle$ are the parts of the amplitude of the $3\pi \to N\tilde{N}$ annihilation process which yield, by analogy with (25), contributions to the Dirac or Pauli form factors, respectively. Conditions (25), (26) are displayed graphically in Figs. 17a and 17b. Let us consider the case of an isovector form factor. Let us assume that the amplitudes $\langle \pi\pi\,|\,T^{+}_{1,2}\,|\,N\tilde{N}\rangle$ can be described well by one resonance wave of the Eq. (14) type. In the limits of very narrow resonance we obtained the following results near resonance from the assumption that $\mathrm{Re} < \pi\pi\,|\,T^{+}_{1,2}\,|\,N\tilde{N} > = 0$ at the resonance point:

$$\langle \pi\pi\,|\,T^{+}_{i}\,|\,N\tilde{N}\rangle \approx \mathrm{Im}\,\langle \pi\pi\,|\,T^{+}_{i}\,|\,N\tilde{N}\rangle \approx \frac{A_i\,(ak^3)^2}{(t_v - t)^2 + (ak^3)^2} \approx \pi A_i\,(ak^3)\,\delta\,(t_v - t)\,^{*}, \tag{27}$$

where $A_i$ is a certain normalization constant; $t_V$ is the resonance position; $a$ is the resonance width. The integration in (23a) can now be carried out in elementary fashion and leads to the result

$$F^{v}_{1,2}(t) = F^{v}_{1,2}(0) + \frac{t\,\mathrm{const}_{1,2}}{t_v - t}. \tag{28}$$

Expression (28) may be rewritten in the form of the well known Clementel-Villi form [29, 30]:

$$F^{v}_{1,2}(t) = F^{v}_{1,2}(0)\left[1 - a^{v}_{1,2} + \frac{t_v}{t_v - t}\,a^{v}_{1,2}\right]. \tag{29}$$

If the presence of strong interaction in the $3\pi$-meson intermediate state is allowed, then by complete analogy with the derivation of Eq. (29) one can obtain the Clementel-Villi form for isoscalar form factors as well:

$$F^{s}_{1,2}(t) = F^{s}_{1,2}(0) + \frac{t\,\mathrm{const}_{1,2}}{t_s - t} \tag{30}$$

*In deriving (27) we used the relationship

$$\delta\,(x - x_0) = \frac{1}{\pi}\lim_{\alpha \to 0}\frac{\alpha}{(x - x_0)^2 + \alpha^2}.$$

or

$$F^s_{1,2}(t) = F^s_{1,2}(0)\left[1 - b^s_{1,2} + \frac{t_s}{t_s - t} b^s_{1,2}\right]. \tag{31}$$

Using Eqs. (28) and (30), it is easy to obtain the expression for the charge form factor of a neutron:

$$F_{1n}(t) = F^s_1(t) - F^v_1(t) = \frac{e}{2} t \left(\frac{b^s_1}{t_s - t} - \frac{a^v_1}{t_v - t}\right).$$

The experimental data indicate the fact that for all values of t the function $F_{1n}(t) \approx 0$, whence we obtain

$$\frac{b^s_1}{t_s - t} - \frac{a^v_1}{t_v - t} \approx 0.$$

Since this relationship is satisfied everywhere, it must also be valid near t = 0, whence we obtain

$$\frac{b^s_1}{t_s} \approx \frac{a^v_1}{t_v} = A.$$

Thus, in order to derive the form factors of nucleons one requires not six parameters ($a^V_1$, $a^V_2$, $t_V$, $b^S_1$, $b^S_2$, $t_S$), as is evident from Eqs. (29), (31), but merely five: A, $a^V_2$, $t_V$, $b^S_2$, $t_S$. Moreover, the position of the resonances $t_V$ and $t_S$ may be taken from experimental data, which reduces the number of independent parameters in the Clementel-Villi model to three.

The principal singularity of the form factors (29) and (31) considered resides in the fact that with increasing transfer t all of them tend to constant limits. This may be interpreted as the presence of a core in the nucleons. It is precisely such an understanding of the problem which existed up to 1962 when experimental data on scattering of electrons by protons and neutrons were known for transfers $q^2 = -t \leq 25^{-2}$ F and were interpreted by means of one vector $\rho$-meson and one scalar meson (see, for example, [31]). However, with increasing energy of the incident electrons in an increase of the transfers $q^2 = -t$ it turned out that the form factor function continued to decrease $\sim 1/q^2$ [32] in such a way that the new data could not be reconciled with the existence of a core in the nucleons. Therefore, it was necessary to reexamine the theoretical interpretation of the results which had been obtained.

## 5. SURVEY OF EXPERIMENTAL DATA ON NUCLEON FORM FACTORS AND THEIR THEORETICAL INTERPRETATION

Problems of the experimental determination of form factors, derivation of the Rosenbluth formula, and the validity of its use in the analysis of experimental data on the scattering of electrons by nucleons have been discussed in detail previously [33]. In this section we shall enumerate only the fundamental experimental data and their interpretation from the modern viewpoint [34-37].

All of the conclusions concerning the behavior of the form factors as functions of the transfer t are based on the Rosenbluth formula [38] for the differential cross section of scattering of electrons by protons ($q^2 = -t$):

$$\frac{d\sigma}{d\Omega} = \sigma_{mo}\left\{F^2_{1p}(q^2) + q^2 F^2_{2p}(q^2) + 2\frac{q^2}{4M^2}[F_{1p}(q^2) + 2MF_2(q^2)]^2 \operatorname{tg}^2\frac{\theta}{2}\right\}, \tag{32}$$

where $\sigma_{mo}$ is the differential cross section of electron scattering by the Coulomb field, while $\theta$ is the scattering angle of an electron in the laboratory coordinate system.

The data on the form factors of a neutron are obtained from experiments on the elastic and inelastic scattering of electrons by deuterons followed by subtraction of the effect of elastic scattering of electrons by protons. A description of this subtraction procedure may be found, for example, in [2, 33].

At present, as a rule, an analysis of the experimental data is carried out by certain combinations of the form factors $F_1^{S,V}$ and $F_2^{S,V}$ rather than by means of the form factors individually:

TABLE 1. Experimental Information on the Functions $G_{Ep}$ and $G_{Mp}$ Obtained for Various Assumptions Concerning the Behavior of $G_{Ep}$ and $G_{Mp}$ for Large Momentum Transfers $q^2$

| $q^2$, $(GeV/c)^2$ | Assumption | $\frac{G_{Ep}}{e}$ | $\frac{G_{Mp}}{e}$ | Upper boundary within the limits of the two standard errors | |
|---|---|---|---|---|---|
| | | | | $\frac{G_{Ep}}{e}$ | $\frac{G_{Mp}}{e}$ |
| 4,87 | $G_{Ep}=0$ | 0 | 0,056 | 0 | 0,076 |
| | $G_{Mp}=0$ | 0,079 | 0 | 0,10 | 0 |
| | $G_{Mp}=(1+\varkappa_p)\,G_{Ep}$ | 0,019 | 0,054 | 0,025 | 0,070 |
| 6,81 | $G_{Ep}=0$ | 0 | 0,038 | 0 | 0,052 |
| | $G_{Mp}=0$ | 0,070 | 0 | 0,097 | 0 |
| | $G_{Mp}=(1+\varkappa_p)\,G_{Ep}$ | 0,013 | 0,037 | 0,018 | 0,051 |

$$G_E=F_1-\frac{q^2}{4M^2}(F_2 2M);\quad G_M=F_1+2MF_2. \tag{33}$$

It can easily be verified that Eq. (32) may be written in especially simple form by means of (33):

$$y=a+bx, \tag{34}$$

where

$$y=\frac{d\sigma}{d\Omega}:\sigma_{mo}\qquad x=\mathrm{tg}^2\frac{\theta}{2};$$
$$a=\frac{G_E^2+\frac{q^2}{4M^2}G_M^2}{1+\frac{q^2}{4M^2}};\qquad b=\frac{q^2}{2M^2}G_M^2,$$

i.e., in the x, y plane the Rosenbluth formula (34) may be represented by a straight line for $q^2$ = const.

There exists still another frequently used notation for the Rosenbluth formula

$$\frac{d\sigma}{d\Omega}=A(\theta,\,t)\,G_E^2+B(\theta,\,t)\,G_M^2, \tag{35}$$

where

$$A(\theta,\,t)=\frac{\sigma_{mo}}{1-\frac{t}{4M^2}};\qquad B(\theta,\,t)=\sigma_{mo}\left(\frac{t}{t-4M^2}-\frac{t}{2M^2}\,\mathrm{tg}\,\frac{\theta}{2}\right),$$

in which the absence of the "interference term" containing the newly determined quantities $G_E$ and $G_M$ [unlike the term $[F_1(q^2)+2MF_2(q^2)]^2$ from Eq. (32)] is clearly emphasized; this leads to a reduction of the correlation errors in isolating the form factors from the experimental data. In the subsequent exposition we shall use only the new form-factor functions $G_E^{S,V}$ and $G_M^{S,V}$ (or $G_{Ep,n}$ and $G_{Mp,n}$).

From Eqs. (33) it follows that:

$$G_{Ep}(0)=F_{1p}(0)=e;\quad G_{En}(0)=F_{1n}(0)=0;$$
$$G_{Mp}(0)=F_{1p}(0)+2MF_{2p}(0)=e(1+\varkappa p)=e\mu_p,\ \mu_p=2.79;$$
$$G_{Mn}(0)=F_{1n}(0)+2MF_{2n}(0)=e\mu_n.$$

The form factor $G_E$ can be normalized to the charge, and therefore it is called the charge form factor, while $G_M$ can be normalized to the total magnetic moment of the nucleons and is called the magnetic form

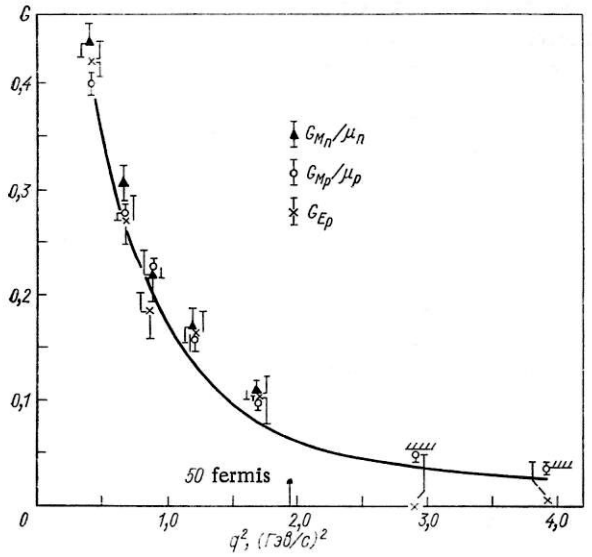


Fig. 18. Comparison of the dipole model for the electromagnetic form factors of nucleons with the experimental data.

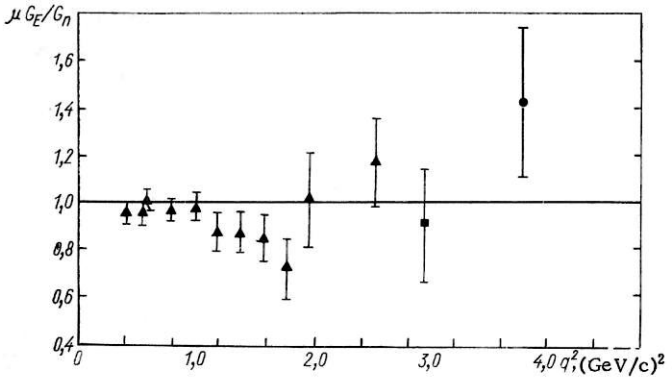


Fig. 19. Check of the deviation from the linear law.

factor. In [34] experimental information on the functions $G_{Ep,n}(q^2)$, $G_{Mp,n}(q^2)$ was obtained up to values $q^2 \approx 3$(GeV/c). Moreover, for the form-factor functions $G_{Ep}$ and $G_{Mp}$ the upper boundaries were obtained for $q^2 = 4.84$ (GeV/c)$^2$ and 6.81 (GeV/c)$^2$, which could simultaneously serve as an estimate of the upper boundary of the core. Due to the smallness of the differential cross section for e + p → e + p scattering at the two values indicated above, it was not possible simultaneously to determine the values of $G_{Ep}$ and $G_{Mp}$ from Eq. (35). Therefore, the analysis was carried out on the assumptions that:

a) if $G_{Ep} = 0$, then $\frac{d\sigma}{d\Omega} = B(\theta, q^2) G_{Mp}^2$;

b) if $G_{Mp} = 0$, then $\frac{d\sigma}{d\Omega} = A(\theta, q^2) G_{Ep}^2$;

c) if $G_{Ep} = \frac{G_{Mp}}{\mu_p} = \frac{G_{Mp}}{1+\varkappa_p}$, then $\frac{d\sigma}{d\Omega} = \left[\frac{A(\theta, q^2)}{(1+\varkappa_p)^2} + B(\theta, q^2)\right] G_{Mp}^2$.

The results of the analysis in [34] are presented in Table 1.

For the form-factor functions $G_{En}$ and $G_{Mn}$ the upper boundary was obtained on the basis of assumptions a-b. For $q^2 = 6.81$ (GeV/c)$^2$ the upper boundary $G_{Mn} = 0.024 \pm \frac{0.012}{0.024}$. For $G_{En}$ the upper boundary was obtained only for $q^2 = 3.89$ (GeV/c)$^2$ and is equal to $0.081 \pm 0.009$.

The experimental data indicate the fact that the neutron form factor $G_{Mn}$ has a behavior similar to the behavior of the form factors $G_{Ep}$ and $G_{Mp}$. A check of the relationships

$$G_{Ep} = \frac{G_{Mp}}{\mu_p} = \frac{G_{Mn}}{\mu_n} = \frac{1}{\left(1+\frac{q^2}{0,71}\right)^2} = G_D, \qquad (36)$$

where $q^2$ is measured in (GeV/c)$^2$, substantiates this (Fig. 18, taken from [34]).

The linear relationship between the form factors $G_{Ep}$, $G_{Mp}/\mu_p$, and $G_{Mn}/\mu_n$, expressed by Eq. (36), is called the scaling law (i.e., a linear law), while the dependence of these form factors on $q^2$ is called the dipole fit (i.e., the dipole model) and in the given review will be designated by the symbol $G_d$. Equation (36) indicates the possibility of describing form factors by means of the one-parameter model.

Recently [37] new data on the proton form factors $G_{Ep}$ and $G_{Mp}$ have been obtained from the $q^2 \leq 25$ (GeV/c)$^2$. In the range of transfers 1 (GeV/c)$^2 \lesssim q^2 \lesssim 2$ (GeV/c)$^2$ a small systematic deviation from the linear law $G_{Ep} = G_{Mp}/\mu_p$ is observed. Figure 19 compares the experimental data with the ratio $\mu_p G_{Ep}/$

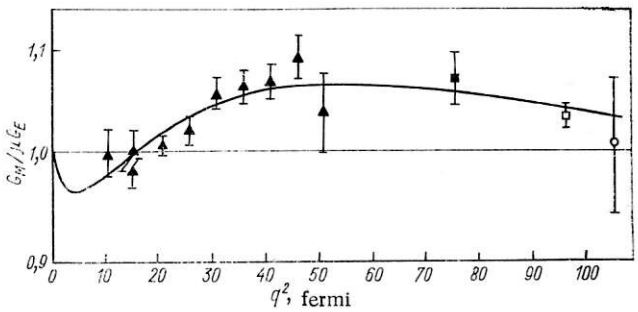


Fig. 20. Comparison of the magnetic form factor of a proton with the dipole model.

TABLE 2. Experimental Information on the Function $(GE_n)^2$

| $q^2$, (GeV/c)$^2$ | $\left(\frac{G_{En}}{e}\right)^2$ | $q^2$, (GeV/c)$^2$ | $\left(\frac{G_{En}}{e}\right)^2$ |
|---|---|---|---|
| 0,389 | +0,026 | 1,17 | −0,012 |
| 0,389 | −0,034 | 1,75 | −0,003 |
| 0,623 | +0,007 | | |
| 0,857 | +0,007 | 2,92 | 0,102 |
| 1,17 | −0,009 | 3,89 | 0,0066 |

$GM_p = 1$ from which it is evident that the deviation is approximately 10%. Figure 20 gives the comparison between the magnetic form factor of a proton and the dipole model. The deviation of the ratio $GM_p/\mu_p G_d$ from unity so far does not have a satisfactory theoretical explanation. Somewhat further on the four-pole model will be discussed, by means of which one can explain the experimental data.

The data on the electrical form factor of a neutron for large transfers are presented in Table 2 (taken from [34]), whence it is evident that $GE_n \approx 0$.

The experimental facts indicate that the form factors $GE_p$, $GM_p$, $GM_n$ decrease with increasing transfer $q^2$ no slower than $1/q^2$. Consequently, if we wish to use the method of dispersion relations for describing the form factors of nucleons, then the dispersion relations for the functions $GE,M$ should be taken without deductions. But this means that the dispersion relations must be taken without deductions for the form factors $F_{1,2}^{S,V}$ also, as is immediately evident from Eqs. (33) for $GE, M$.* We see that the language of dispersion relations is convenient for the theoretical interpretation of experimental data.

However, before writing the dispersion relations for the functions G let us note a certain fact. Having solved Eq. (33) for $F_1$, we obtain:

$$\left.\begin{aligned} F_1(t) &= \frac{G_E(t) - \frac{t}{4M^2} G_M(t)}{1 - \frac{t}{4M^2}}; \\ F_2(t) &= \frac{G_M(t) - G_E(t)}{2M\left(1 - \frac{t}{4M^2}\right)}, \end{aligned}\right\} \tag{37}$$

whence it is evident that at the point $t = 4M^2$ (i.e., at the physical threshold of the annihilation channel) the denominator $1 - \frac{t}{4M^2}$ vanishes. Thus, the functions $F_{1,2}(t = 4M^2)$ go to infinity if it is not assumed that $GM(4M^2) = GE(4M^2)$. We shall assume that such an equation exists, and we write the dispersion relations under these conditions.

Thus,

$$G_{E,M}^{v}(t) = \frac{1}{\pi} \int_{4m_\pi^2}^{\infty} \frac{\operatorname{Im} G_{E,M}^{v}(t')}{t' - t} dt'. \tag{38}$$

Analogous dispersion relations can be written for the functions $G_E^S$ and $G_M^S$, the only difference being that the lower limit begins at $m_\pi^2$. The unitarity condition for $\operatorname{Im} G_{E,M}^{S,V}$ is graphically depicted just as it is in Fig. 17. Let us assume that the spectral functions $\operatorname{Im} G_{E,M}^{S,V}$ may be represented in the form of a sum of $\delta$-like terms (in the previous section the spectral functions $\operatorname{Im} F_{1,2}^{S,V}$ were approximated by one $\delta$-function):

*In [35] the authors showed that the dispersion approach is identically good for application to both the functions GE and GM and the functions $F_1$, $F_2$.

TABLE 3. Values of the Parameters $\alpha_i$, $\beta_i$ and the Core in Models b-d

| Model | $I=1$ | | | $I=0$ | | | $I=1$ | | | $I=0$ | | |
|---|---|---|---|---|---|---|---|---|---|---|---|---|
| | $\alpha_1$ | $\alpha_2$ | core | $\alpha_3$ | $\alpha_4$ | core | $\beta_1$ | $\beta_2$ | core | $\beta_3$ | $\beta_4$ | core |
| б | 0,5 | 0 | — | 1,477 | —0,977 | — | 2,353 | 0 | — | 1,612 | —1,172 | — |
| в | 0,525 | 0 | —0,025 | 1,090 | —0,555 | —0,035 | 2,471 | 0 | —0,118 | 1,060 | —0,594 | —0,031 |
| г | 2,347 | —1,847 | — | 1,214 | —0,714 | — | 8,268 | —5,915 | — | 1,093 | —0,653 | — |

$$\left.\begin{aligned} \operatorname{Im} G_E^{v,s}(t) &= \sum_i \alpha_i \pi \delta(t-t_i); \\ \operatorname{Im} G_M^{v,s}(t) &= \sum_i \beta_i \pi \delta(t-t_i), \end{aligned}\right\} \tag{39}$$

where $\alpha_i$, $\beta_i$ are constants which must be calculated theoretically and must depend on the interaction parameters $\pi$ as other particles with nucleons, while $t_i = M_i^2$ are the positions of the isovector or isoscalar mesons which yield the contribution to the form-factor function G by assumption. Having substituted Eqs. (39) into (38), we obtain:

$$\left.\begin{aligned} G_E^{v,s}(t) &= \sum_i \frac{\alpha_i}{1-\frac{t}{M_i^2}}; \\ G_M^{v,s}(t) &= \sum_j \frac{\beta_j}{1-\frac{t}{M_j^2}}. \end{aligned}\right\} \tag{40}$$

None of the form-factor functions (40) have a core, and for $t \to \infty$ all of them decrease according to the law $\sim 1/q^2$. If one of the meson masses (or several of them) turns out to be very large, then in this case the form-factor functions (40) can simulate the existence of a core.

Let us make use of the relations

$$\begin{aligned} G_{E_p} &= G_E^s + G_E^v; \quad G_{M_p} = G_M^s + G_M^v; \\ G_{E_n} &= G_E^s - G_E^v; \quad G_{M_n} = G_M^s - G_M^v, \end{aligned}$$

and let us write the proton form factors in explicit form:

$$\left.\begin{aligned} G_{E_p} &= \frac{\alpha_1}{1+\frac{q^2}{M_{1v}^2}} + \frac{\alpha_2}{1+\frac{q^2}{M_{2v}^2}} + \frac{\alpha_3}{1+\frac{q^2}{M_{3s}^2}} + \frac{\alpha_4}{1+\frac{q^2}{M_{4s}^2}} + \dots \\ G_{M_p} &= \frac{\beta_1}{1+\frac{q^2}{M_{1v}^2}} + \frac{\beta i}{1+\frac{q^2}{M_{2v}^2}} + \frac{\beta_3}{1+\frac{q^2}{M_{3s}^2}} + \frac{\beta_4}{1+\frac{q^2}{M_{4s}^2}} + \dots \end{aligned}\right\} \tag{41}$$

In the notation (41) the contributions from isovector or isoscalar mesons are marked by the symbol v or s used as a subscript for the masses (i.e., $M_S$ or $M_V$); i.e., the contribution from two isovector and two isoscalar mesons are written out in explicit form. The neutron form factors differ from the notation (41) in that they have opposite signs which appear before the contributions from isovector mesons.

In order to analyze the experimental data one may choose the one-pole, two-pole, three-pole, etc., approximations. At present three mesons are known: one isovector meson (a $\rho$-meson), and two isoscalar mesons ($\omega$ and $\varphi$) each of which may make a contribution to the form factors of the nucleons in accordance with the unitarity conditions (25)-(27) and (39). In [34] an analysis is carried out for the following possible cases:

a) the dipole model in accordance with Eq. (36);

b) the three-pole approximation as the one which most completely considers the contribution from all known mesons and having no core;

c) the three-pole approximation – with a core;

d) the four-pole approximation if none of the previous ones provides satisfactory agreement with the experimental data.

For the time being it is inexpedient to use more complex models to explain the nucleon form factors.

The dipole approximation is very attractive due to its exceptional simplicity. It may also be interpreted as the two-pole approximation with close values of masses corresponding to the resonances and coupling constants having opposite signs. Comparisons with experimental data are presented in Fig. 18.

The three-pole approximation (with or without the core) likewise can provide good agreement with experimental data. However, under these conditions it leads to the necessity of taking underestimated values of the $\rho$-meson mass.

In [35, 36] the proton and neutron form factors were measured and analyzed in the range $q^2 \leq 30\ F^{-2}$.

In the three-pole model the authors obtained the following expressions for the isoscalar and isovector parts of the nucleon form factors:

$$\left.\begin{aligned}
G_E^s &= 0.5e\left\{\frac{2.18\pm0{,}06}{1+\frac{q^2}{15.7}}-\frac{1.11\pm0.14}{1+\frac{q^2}{26.7}}-0.07\pm0{,}15\right\};\\
G_M^s &= 0.44e\left\{\frac{2.42\pm0.05}{1+\frac{q^2}{15.7}}-\frac{1.35\pm0.09}{1+\frac{q^2}{26.7}}-0.07\pm0.15\right\};\\
G_E^v &= 0.5e\left\{\frac{1.05\pm0.07}{1+\frac{q^2}{(7.51\pm0.32)}}-0.05\pm0.07\right\};\\
G_M^v &= 2.353e\left\{\frac{1.05\pm0.01}{1+\frac{q^2}{(7.51\pm0.32)}}-0.05\pm0.01\right\}.
\end{aligned}\right| \qquad (42)$$

From Eqs. (42) it follows that in the range of small $q^2$:

1) the constant terms are close to zero;

2) the $\rho$-meson mass is approximately 200 MeV below the value observed ($M_\rho = 548 \pm 24$ MeV). In order to improve the agreement with respect to the $\rho$-meson mass, the authors proposed the existence of still another vector meson (a B-meson having a mass of 1220 MeV and a width of 100 MeV [39]) and used the four-pole approximation.

For higher transfers $q^2$ the interpretation of the form factors remains the same. A check of Eq. (41) showed that if known masses of the isoscalar mesons $\varphi$ and $\omega$ are specified, while the $\rho$-meson mass is made variable, then the best fit to the experimental data is achieved for the value $M_\rho = 510$ MeV in the b model, while in the c model it is achieved for the value $M_\rho = 540$ MeV. The best agreement with experimental data (according to the $\chi^2$-estimate) can be achieved in the d model with two isovector and two isoscalar mesons. The values of the masses of the $\rho$-, $\omega$-, and $\varphi$-mesons are chosen from experiments. The value of the mass of the vector meson is the fit parameter. In Table 3 the parameters of approximations b-d) are written out. The parameter of the approximation $a$ is indicated in Eq. (36). The mass of the second vector meson in the d model is $M_{\rho'} = 875$ MeV. Figures 21 to 24 demonstrate the comparison of the approximations $a$, c, d with the experimental data for $G_{E_p}$, $G_{M_p}$, $G_{M_n}$, and $G_{E_n}$ respectively (Figs. 21-24 taken from [34]).

In [40] the authors stated the purpose of using the four-pole model to describe the form-factor functions of a proton with allowance for deviation from the linear law governing the behavior of the form factor:

$$G_{E_p}(q^2) = \sum_{i=1}^{4} \frac{A_i}{M_i^2 + q^2}, \qquad (43)$$

where $M_1$ is a fictitious pole which considers the contribution of the continuous spectrum which causes an abrupt drop at $q^2 = 0$ ($M_1 = 0.45$ GeV); $M_2$ is the mass of a $\rho$-meson; $M_3$ is the mass of a hypothetical $\rho'$-

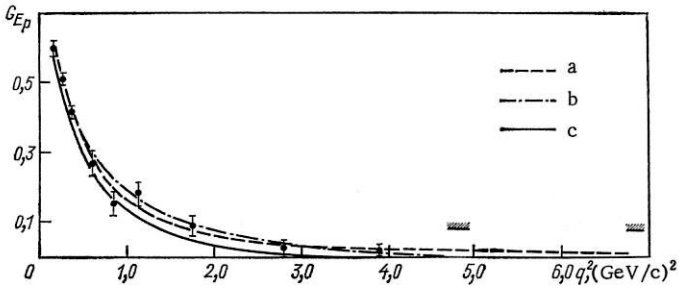


Fig. 21. Comparison of the approximations (or models) *a*, c, and d for the function $GE_p$ with the experimental data.

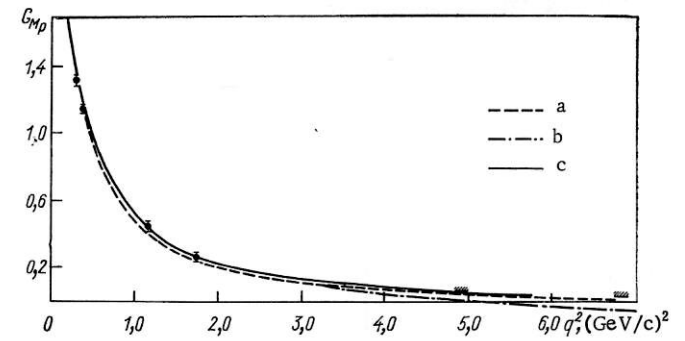


Fig. 22. Comparison of the approximations (or models) *a*, b, and d for the function $GM_p$ with experimental data.

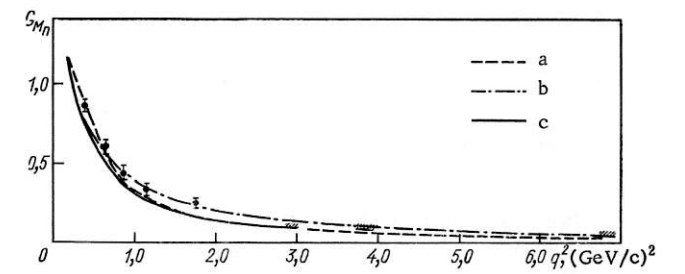


Fig. 23. Comparison of the approximations (or models) *a*, b, and d for the function $GM_n$ with experimental data.

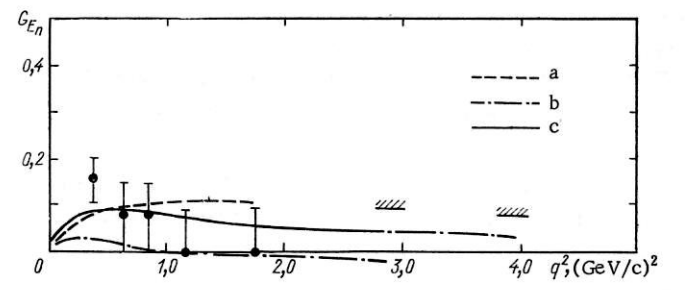


Fig. 24. Comparison of the approximations (or models) *a*, c, and d for the function $GE_n$ with experimental data.

meson [41] which is equal to 1.31 GeV; $M_4$ is the fictitious pole which considers the contribution of the far singularities in the dispersion integral and causes a drop of the form factor for large transfers ($M_4$ = 2.456 GeV). For such a set of masses, the constants $A_i$ take the values: $A_1 = 0.047$, $A_2 = 0.834$, $A_3 = -1.263$, $A = 0.446$.

Figure 25 gives a comparison of the theoretical curve (43) with the experimental data ($GE_p/G_D = 1$). Notwithstanding the clear physical meaning of the representation (43), it nevertheless cannot be considered satisfactory due to the large number of arbitrary parameters.

At the end of this section we shall discuss exponential models of form factors proposed in [42-45].

It is well known that the microcausality principle allows exponential growth of the amplitude at infinity; however, this growth must be slower than a linear exponential. In this case one may not write the dispersion relation with a finite number of deductions, as is done for the amplitudes having polynomial growth.

Logunov, Mestvirishvili, and Sillen [42] considered the class of functions which allows a nonpolynomial growth of the amplitude at infinity and is convenient for describing the experimental data. Assume the function G(t) is the form factor function of a nucleon having the cut $0 < a \leqslant t \leqslant +\infty$. The t-plane is converted into a unit circle by means of the conformal transformation

$$\xi = \frac{\sqrt{a} - \sqrt{a-t}}{\sqrt{a} + \sqrt{a-t}},$$

so that $G(t) \to f(\xi)$.

Assume $f(\xi) \in A$, where A is the class of all functions which are analytic in the unit circle and satisfy the condition:

$$\lim_{\rho \to 1} \int_0^{2\pi} \ln^+ |f(\rho e^{i\theta})| \, d\theta \leqslant A < \infty,$$

where

$$\ln^+ a = \begin{cases} \ln a & a \geqslant 1 \\ 0 & a < 1. \end{cases}$$

Such a representation allows a fairly varied behavior at infinity for G(t). However, this is only a minimal extension in comparison with the polynomial-growth function. Functions from the class A may be represented in the form

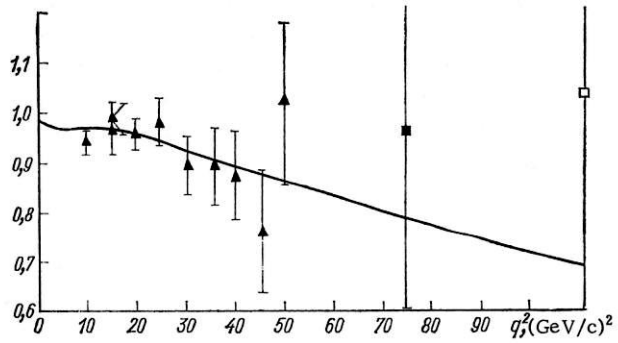


Fig. 25. Comparison of the ratio of the function $G_{Ep}$ obtained from Eq. (43) to the function $G_D$ with experimental data.

$$f(\xi) = b(\xi)\, e^{\Phi(\xi)},$$

where $b(\xi)$ is a Bliascshke function, while $\Phi(\xi)$ has the form

$$\Phi(\xi) = i\Phi(0) + \frac{1}{2\pi i}\int\limits_{|z|=1} \frac{\omega(z)}{z-\xi}\,dz,$$

where $\omega(z)$ is the discontinuity of the function on the cut.

Returning now to the variable t, we obtain

$$b(\xi) = B(t)\, e^{g(t)} \text{ and } G(t) = B(t)\, e^{g(t)+\varphi(t)},$$

where $\varphi(t)$ is the transform of $\Phi(\xi)$ in the t plane, while g(t) is a function having a cut in the t plane $t(a \leq t \leq \infty)$. If it is assumed that B(t) has a finite number of zeros (we shall not consider the case of an infinite number here), then a representation in the form

$$G(t) = B(t) \exp\left[\frac{1}{\pi}\int\limits_0^\infty \frac{\operatorname{Im} g(t')\,dt'}{t'-t} + \frac{t-a}{\pi}\int\limits_a^\infty \frac{\operatorname{Im}\varphi(t')\,dt'}{t'-t} + \varphi(a)\right]$$

is obtained for the form-factor function G(t). Now one can find Img(t) and Im$\varphi$(t) by extrapolation of experimental data (i.e., the imaginary parts of the proton form factors $G_{Ep}$ and $G_{Mp}$) in the time-like domain of the momentum t.

Let us suppose that B(t) = 1. This assumption can be justified by the fact that the function $e^{g(t)+\varphi(t)}$ provides a good description of the experimental data on the nucleon form factors in the domain of space-like momentum transfers. Let us also consider the additional information:

$$G_{E_p}(0) = 1; \quad G_{M_p}(0) = 2.79;$$
$$G_{E_p}(4M^2) = G_{M_p}(4M^2); \quad G_{E_p}(-\infty) = G_{M_p}(-\infty) = 0.$$

Let us choose the following approximating expressions:

$$G_{E_p} = \exp\left[\frac{a_0\xi}{1+\xi} + a_1\xi + a_2\xi^2\right];$$
$$G_{M_p} = \exp\left[\frac{b_0\xi}{1+\xi} + b_1\xi + b_2\xi^2\right].$$

After the coefficients $a_i$ and $b_i$ have been found according to the experimental data in the $t < 0$ domain, the expressions $G_{Ep}$ and $G_{Mp}$ may be continued analytically in the time-like domain of transfers t. In this domain $\operatorname{Im}G_{Ep}$ and $\operatorname{Im}G_{Mp}$ oscillate, and these oscillations may be detected experimentally for measurement of the polarization in the $p + \bar{p} \to e^+(\mu^+) + e^-(\mu^-)$ reaction.

Using the method of analytic continuation, one could hope to obtain the positions and widths of the well-known resonances $\rho$, $\omega$, $\varphi$ from oscillations of $\operatorname{Im}G_{Ep}$ and $\operatorname{Im}G_{Mp}$ in the domain $t > 4m_\pi^2$. The authors, regrettably, were not able to obtain the correct values of the parameters of the resonances enumerated above. It should, however, be noted that in [42] not all the possibilities inherent in the model were used, since only the case B(t) = 1 was considered.

In [43] the authors started from experimental data on the scattering of protons by protons at high energies and high momentum transfers. The behavior of the differential cross sections of p + p → p + p can be described by the exponential Orear formula:

$$\frac{d\sigma}{d\Omega}(\theta, p_\perp) \sim Ce^{-\frac{p_\perp}{0.15}},$$

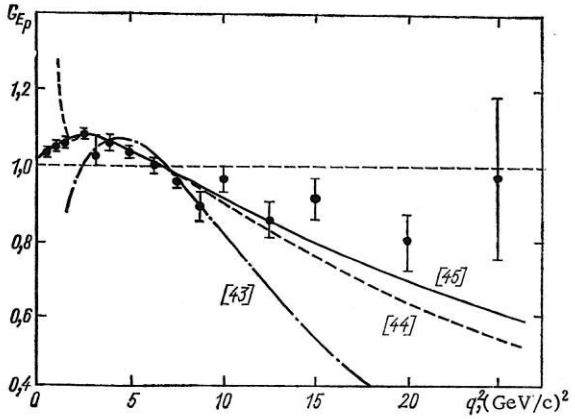


Fig. 26. Comparison of various experimental representations for the proton form factors with experimental data.

where C is a certain constant, while $p_\perp$ is the transverse momentum transfer. Wu and Yang made the natural assumption that in elastic e + p → e + p-scattering there must be a rapid drop of the differential cross section, which is of the exponential type, and such behavior may occur as a result of the exponential behavior of the proton form factor functions:

$$\left.\begin{aligned} G(q^2) &\sim Be^{-\frac{p_\perp}{p_0}};\\ G_{M_p} &= \mu_p G_{E_p}, \end{aligned}\right\} \qquad (44)$$

where $p_\perp$ should be replaced by $\sqrt{q^2}$ and $p_0$ is a certain constant which is chosen from experimental data. It is assumed that the factor B may be a constant or may depend weakly on $q^2$.

Actually the form factors (44) provide a fairly good description of the experimental data for the value $p_0$ = 0.6 (GeV/c) and B = const. However, one should note two singularities of these form factors.

1. Their analytic properties are false, since the cross section of the functions $G(q^2)$ begins with the values t = 0 rather than with the values $t = 4m_\pi^2$, as derives from a field-theory consideration. This shortcoming is easily corrected. It is sufficient to replace $\sqrt{q^2}$ for the function $\sqrt{q^2 + 4m_\pi^2}$:

$$G(q^2) = Be^{-\frac{\sqrt{q^2+4m_\pi^2}}{0.6}}/e^{-\frac{2m_\pi}{0.6}}.$$

2. As has already been said above in analyzing the paper by Logunov et al. [42], the exponent in the time-like domain $q^2 < 0$ becomes imaginary and the form factor function (44) begins to oscillate so as to give equally spaced minima and maxima in $G(q^2)$. Such a behavior differs from the behavior of the four-pole approximation in the time-like intervals of $q^2$ and provides the possibility of choosing one of the models named here by comparison with experimental data on annihilation:

$$e^+ + e^- \rightarrow N + \bar{N}.$$

In [44] a form factor of the form

$$\frac{G_{M_p}}{\mu_p} = 27.8\exp\left[-\sqrt{\frac{q}{0.040}}\right] \qquad (45)$$

was proposed, while in [45] an exponential form factor with the asymptotic behavior

$$\frac{G_{M_p}}{\mu_p} \sim e^{-A\ln^2(aq^2)} \qquad (46)$$

was proposed, where A and $a$ are fitting constants.

A comparison of Eqs. (44)-(46) with experimental data is given in Fig. 26. It is evident that the exponential form factors may describe experimental data only in a certain portion of the transfers $q^2$.

## LITERATURE CITED

1. R. Hofstadter, Nuclear and Nucleon Structure. A Collection of Reprints with an Introduction, W. A. Benjamin, New York (1963).
2. S. D. Drell and S. Zachariasen, Electromagnetic Structure of Nucleons, Oxford University Press, Oxford (1961) [Russian translation: Moscow, Izd. Inostr. Lit. (1962)].

3. Michel Gourdin, Herzeg Novi Lectures, 1961, Vol. 2. Lectures on High-Energy Physics (Sixth Summer Meeting, Herzeg Novi), Gordon and Breach (1965).
4. L. N. Hand, D. G. Miller, and R. Wilson, Rev. Mod. Phys., 35, 335 (1963).
5. H. J. Bremmerman, R. Oehme, and J. G. Taylor, Phys. Rev., 109, 2178 (1968).
6. W. Paull, Rev. Mod. Phys., 13, 203 (1941).
7. S. M. Bilenky, et al., Nucl. Phys., 7, 646 (1958).
8. Y. Nambu, Nuovo Cimento, 6, 1064 (1957).
9. N. I Muskhelishvili, Singular Integral Equations, 2nd ed. [in Russian], Fizmatgiz, Moscow (1962); R. Omnes, Nuovo Cimento, 8, 316 (1968).
10. P. S. Isaev and V. A. Meshcherakov, Zh. Éksperim. i Teor. Fiz., 43, 1339 (1962). P. S. Isaev, V. I. Lend'el, and V. A. Meshcherakov, Zh. Éksperim. i Teor. Fiz., 45, 294 (1963).
11. J. Bowcock, W. N. Cottingham, and D. Lurie, Nuovo Cimento, 16, 918 (1960).
12. L. A. Khalfin and Yu. B. Shcherbin, Pis'ma Zh. Éksperim. i Teor. Fiz., 8, 588 (1968); 8, 642 (1968).
13. Yu. P. Shcherbin, Pis'ma Zh. Éksperim. i Teor. Fiz., 10, 340 (1969).
14. A. V. Efremov, Zh. Éksperim. i Teor. Fiz., 53, 732 (1967).
15. E. G. Grishin, É. P. Kistenev, and Mu Tsyun, Yadernaya Fizika, 2, 886 (1965).
16. C. W. Akerlov, et al., Phys. Rev., 163, 1482 (1957).
17. D. Yu. Bardin, et al., Communications of the Joint Institute for Nuclear Research, E1-4786, Dubna (1969).
18. D. Yu. Bardin, V. B. Semikov, and N. M. Shumeiko, Yadernaya Fizika, 10 (1969); Preprint of the Joint Institute for Nuclear Research R-4-4532, Dubna (1969).
19. T. Kahane, Phys. Rev., 135, B975 (1964).
20. V. L. Auslender, G. I. Budker, et al., Phys. Lett., 25B, 433 (1967).
21. V. L. Auslender, G. I. Budker, et al., Yadernaya Fizika, 9, 114 (1969).
22. J. Augustin, J. Bizot, et al., Phys. Lett., 28B, 508 (1969).
23. R. Perez-y-Torba, Fourth International Symposium on Electron and Photon Interaction at High Energies, Liverpool (1968).
24. S. K. Smirnov, Diplomate Paper, Moscow State University, Technical Physics Laboratory of the Joint Institute for Nuclear Research (1969).
25. V. A. Riazzudin, Phys. Rev., 114, 1184 (1959).
26. Y. Tanaka, Nuovo Cimento, A60, 589 (1969).
27. G. M. Zinov'ev and B. V. Struminskii, Yadernaya Fizika, 9, 173 (1969).
28. V. I. Ogievetskii and Chou Huan-Chao, Zh. Éksperim. i Teor. Fiz., 37, 866 (1969).
29. E. Clementel and E. Villi, Nuovo Cimento, 4, 1207 (1956).
30. S. Bergia et al., Phys. Lett., 6, 367 (1961).
31. R. Hofstadter and R. Hermann, Phys. Rev. Lett., 6, 293 (1961).
32. K. W. Chen, et al., Phys. Rev. Lett., 11, 561 (1963).
33. A. Verganelakis, Electromagnetic Form Factors, Ecole Internationall de la Physique des Particles Elementairer, Herzeg Novi (Yugoslavia) (1965).
34. L. H. Chan, et al., Phys. Rev., 141, 1298 (1966).
35. E. B. Hughes, et al., Phys. Rev., 139, B458 (1965).
36. T. Janssens, et al., Phys. Rev., 142, 922 (1966).
37. J. G. Rutherglen, Fourth International Symposium on Electron and Photon Interactions at High Energies, Liverpool. Daresbury Nuclear Physics Laboratory (1969). (This review paper contains references to experimental papers on the measurement of nucleonic form factors, which were performed on the DESY, Bonn, and SLAC accelerators in 1967-1969).
38. M. N. Rosenbluth, Phys. Rev., 79, 615 (1950).
39. M. Abolins et al., Phys. Rev. Lett., 11, 381 (1963).
40. Ch. Berger et al., Electromagnetic Form Factors of a Proton between 10 and 50 $F^{-2}$, Physikalisches Institute, University of Bonn, Preprint 1-075, July (1969).
41. C. Lovelace, Phys. Lett., 28B, 264 (1968).
42. A. A. Logunov, M. A. Mestvirishvili, and I. N. Silin, Preprint of the Joint Institute for Nuclear Research R-2519, Dubna (1965).
43. T. T. Wu and C. N. Yang, Phys. Rev., 137B, 708 (1965).
44. S. D. Drell, A. C. Finn, and M. H. Goldhaber, Phys. Rev., 157, 1402 (1967).
45. G. Mack, Phys. Rev., 159, 1615 (1967).
46. D. H. Coward, et al., Phys. Rev. Lett., 20, 292 (1968).